

Attakolite: New data and crystal-structure determination

JOEL D. GRICE

Mineral Sciences Section, Canadian Museum of Nature, Ottawa, Ontario K1P 6P4, Canada

PETE J. DUNN

Department of Mineral Sciences, Smithsonian Institution, Washington, DC 20560, U.S.A.

ABSTRACT

Attakolite, a silico-phosphate mineral from the Västana mine, Sweden, has been submitted to chemical and X-ray structure analysis in order to establish its crystal structure and chemical formula. The mineral is monoclinic, space group $C2/m$, with cell parameters refined from X-ray powder diffraction; $a = 17.188(4)$, $b = 11.477(8)$, $c = 7.322(5)$ Å and $\beta = 113.83(4)$. Complete X-ray powder diffraction and optical data are given. An electron microprobe analysis gave SiO₂ 5.9, P₂O₅ 33.6, Al₂O₃ 26.8, Fe₂O₃ 3.9, MnO 9.7, CaO 6.6, SrO 3.0, and H₂O (difference) 10.5. This analysis in conjunction with the crystal-structure determination yields the simplest formula, (Ca,Sr)Mn(Al,Fe³⁺)₄[HSiO₄][PO₄]₃(OH)₄, with $Z = 4$. The structure has been refined to $R = 2.6\%$ and $R_w = 2.3\%$. The layer composed of chains of [AlO₄(OH)₂] octahedra with independent [PO₄] and [SiO₃(OH)] tetrahedra in attakolite is compared with similar structural features in carminite, palermoite, tsumcorite, and the desclozite and adelite groups. As the silicate anion is a stronger Lewis base than the phosphate anion, it predictably is the hydrogenated anionic species.

INTRODUCTION

During an investigation of silico-phosphate minerals, the authors noted some inconsistencies in the composition of attakolite when compared with the chemical analyses presented in the original description of the species by Blomstrand (1868) and in the more recent data of Gabrielson and Geijer (1965). Also, there are differences between the crystal structure reported by Gabrielson and Geijer (1965) and that presented by Mead and Mrose (1968), which required further study. To date, attakolite has been reported from only one locality, the Västana mine, near Näsund, Kristianstad, Sweden. In the present research project two specimens from the Smithsonian Institution's collection were used, one of which (R5615) was part of the study by Mead and Mrose (1968). This specimen was used for the optical data and crystal structure determination, but chemical analyses of both are given. The changes presented here for the crystallographic data and the chemical formula of attakolite have been approved by the IMA Commission on New Minerals and Mineral Names.

Although attakolite seems to be very rare in world occurrences, at the Västana mine itself it appears to have been quite common (Gabrielson and Geijer, 1965). There it is associated with quartz, apatite, hematite, lazulite, svanbergite, and pyrophyllite.

PHYSICAL AND OPTICAL PROPERTIES

Attakolite is massive to granular, ranging in color from white to pink. Optical properties were measured for comparison with those of Mrose (Palache et al., 1951). In

general, the two sets of optical properties compare well, but the refractive indices reported here are somewhat lower. Optically, attakolite is clear and colorless with no apparent absorption or pleochroism but with a strong dispersion $r \gg v$. The mineral is biaxial, positive, $2V_{\text{meas}} = 75^\circ \pm 5^\circ$, $2V_{\text{calc}} = 74^\circ$, $\alpha = 1.650(1)$, $\beta = 1.654(1)$, and $\gamma = 1.661(1)$, as determined in Na light. The orientation is $Y = b$, $Z = c$, and $X \wedge a = +24^\circ$ (in β obtuse).

CHEMICAL COMPOSITION

Attakolite was chemically analyzed using an ARL-SEMQ electron microprobe utilizing a 15-kV operating voltage and a sample current of 0.025 μA , measured on brass. Standards used were hornblende (Si, Fe), scapolite (Al), fluorapatite (Ca, P), manganite (Mn), and celestine (Sr). A wavelength-dispersive microprobe scan indicated the absence of other detectable elements. The studied sample was homogeneous. The data were corrected using a modified version of the Magic-4 program, and the results are presented in Table 1. Fe was calculated as Fe³⁺ in part on the basis of closely associated hematite, the deficiency of Al, and the implications of the crystal-structure determination.

Gabrielson and Geijer (1965) proposed the general formula, $X_3Y_6[Z(O,OH)_4]_3 \cdot 3H_2O$ with $Z = 4$, based on their empirical formula $(\text{Ca}_{2.01}\text{Sr}_{0.32}\text{Mn}_{0.69})_{23}(\text{Al}_{5.28}\text{Fe}_{0.27}\text{Mn}_{0.38}\text{Mg}_{0.07})_{26}[(\text{P}_{4.83}\text{Si}_{1.64}\text{Al}_{0.24})_{26.71}(\text{O}_{26.84}\text{OH}_{1.22})_{28.06}] \cdot 2.80\text{H}_2\text{O}$. This empirical formula was calculated utilizing the unit-cell volume and density. Gabrielson and Geijer (1965) were careful to point out that "the evidence at hand does not permit any definite conclusions as to the

TABLE 1. Chemical composition of attackolite

	R5615	135693	Blix*	Calc**
SiO ₂	5.9	7.9	9.35	6.18
P ₂ O ₅	33.6	31.9	32.48	35.01
Al ₂ O ₃	26.8	26.7	26.72	27.89
Fe ₂ O ₃	3.9†	2.6†	2.05	3.93
MnO	9.7	10.5	7.10	10.57
CaO	6.6	7.8	10.67	6.77
SrO	3.0	1.1	3.15	2.93
H ₂ O	[10.5]‡	[11.5]‡	5.83	6.71
Total	100	100	97.64	100
Cation proportions based on 20 O atoms				
Si	0.68	0.91	1.07	0.69
P	3.28	3.12	3.12	3.31
Al	3.65	3.64	3.57	3.67
Fe ³⁺	0.34	0.22	0.18	0.33
Mn	0.95	1.03	0.68	1.00
Ca	0.81	0.97	1.30	0.81
Sr	0.20	0.07	0.21	0.19
H	8.08	8.86	4.41	5.00

* R. Blix analyst (Gabrielson and Geijer, 1965), also MgO 0.29 wt%.

** Calculated from atomic proportions used in crystal structure analysis.

† Total Fe calculated as Fe₂O₃.

‡ H₂O by difference.

TABLE 2. Comparison of attackolite unit cells

	Present study	Gabrielson*	Mead**	Mead**
Symmetry	Monoclinic	Orthorhombic	Monoclinic	Orthorhombic
<i>a</i> (Å)	17.188(4)	11.38(<i>b</i>)	11.45(<i>b</i>)	11.46
<i>b</i> (Å)	11.477(8)	13.22(2 <i>d</i> ₀₁)	15.69(<i>d</i> ₁₀₀)	15.71
<i>c</i> (Å)	7.322(5)	14.08(5 <i>d</i> ₀₁)	7.30(<i>d</i> ₀₁)	7.28
β (°)	113.83(4)	90(≈90)	91.5(91.5)	90

Note: The values in parentheses in the last three columns give setting compared to present study.
* Gabrielson and Geijer (1965).
** Mead and Mrose (1968).

presented below, establish the centrosymmetric space group *C2/m* as the correct choice. Unit-cell parameters were refined from X-ray powder diffraction data obtained with a Gandolfi camera 114.6 mm in diameter with CuKα radiation (Table 3).

CRYSTAL-STRUCTURE DETERMINATION

For the intensity data measurement, a reasonably equant grain (0.12 mm in diameter) of attackolite was chosen. Intensity data were obtained using a fully automated, Nicolet R3*m* four-circle diffractometer operated at 50 kV and 35 mA with graphite-monochromated MoKα radiation. A set of 25 reflections was used to orient the crystal and refine the cell dimensions: *a* = 17.210(4), *b* = 11.507(3), *c* = 7.310(1) Å, and β = 113.87(2)° and *V* = 1323.9(5) Å³. A unique set of intensity data up to 2θ = 60° was collected. Of the 2102 intensities obtained, 1681 were considered observed [*F* > 4σ(*F*)].

Reduction of the intensity data and solution and refinement of the structure were done by the SHELXTL package of programs (Sheldrick, 1990). Data reduction included background, scaling, Lorentz and polarization, and absorption corrections. For the absorption correction, 11 intense diffraction maxima over the 2θ range 9–60° were chosen for ψ-diffraction-vector scans after the method of North et al. (1968). The ψ-scan set of intensity data was used to refine an ellipsoidal, empirical absorption correction with μ = 30 cm⁻¹. Absorption correction reduced the merging *R* of the ψ-scan data set from 1.8 to 1.4%, which, when applied to the whole data set, resulted in relative minimum and maximum transmissions of 0.750 and 0.829. Scattering curves for neutral atoms from Cromer and Mann (1968) and anomalous dispersion coefficients from Cromer and Liberman (1970) were used in conjunction with the weighting scheme $R_w = \Sigma \sqrt{w}(|F_o| - |F_c|) / \Sigma \sqrt{w} F_o$ with *w* = 1.

The mean value of |*E*² - 1| is 0.982, which favors the centrosymmetric space group *C2/m*. Phasing of a set of normalized structure factors gave a model with 16 peaks. This initial model, with the appropriate assignment of scattering factors, refined to give a residual index *R* = 22%. Subsequent refinement, combined with difference Fourier maps, resulted in location of the six remaining O atoms. With all atoms except H, the structure refined to

chemical formula.” In the present study the simplest formula, XYZ₄(HSiO₄)(PO₄)₃(OH)₄ with Z = 4, is based on the crystal-structure determination, since the chemical-analytical data of specimen NMNH R5615 (Table 1), for which the crystal structure was determined, yields the empirical formula, (Ca_{0.81}Sr_{0.20})_{Σ1.01} Mn_{0.95} (Al_{3.65}Fe_{0.34})_{Σ3.99} [H(Si_{0.68}P_{0.28})O₄](PO₄)₃(OH)₄ based on 20 O atoms.

X-RAY CRYSTALLOGRAPHY

Attackolite was reported as orthorhombic by Gabrielson and Geijer (1965), but they were unable to find suitable crystals for single-crystal X-ray diffraction studies; hence their choice of symmetry was based on optical data, and they were able to refine a reasonable set of unit-cell parameters (Table 2) using their X-ray powder-diffraction data. Mead and Mrose (1968) reported two closely related unit cells (Table 2) on the basis of a single-crystal X-ray study. They found the white grains to be monoclinic and the pink grains to be orthorhombic. They did not attempt to relate their orthorhombic cell to that of Gabrielson and Geijer (1965). In the present study, the same sample (NMNH R5615) utilized by Mead and Mrose was used, but the present authors could not confirm their exact findings. Their “monoclinic” setting was found but it did not have a monoclinic diffraction aspect. The authors did not observe Mead and Mrose’s orthorhombic attackolite, but it is interesting to note that Gabrielson and Geijer (1965) report that “a lamellar structure, which probably is caused by twinning” was seen in thin sections of attackolite. Both planes (100) and (101) of the present setting are pseudomirror planes. If either of these were a twin plane, a pseudoorthorhombic cell of the type reported by Mead and Mrose (1968) would result.

The authors’ precession studies show attackolite to be monoclinic, with possible space group choices *C2/m*, *C2*, and *Cm*. Results of the crystal-structure determination,

TABLE 3. X-ray powder diffraction data for attakolite

l_{obs}	d_{obs}	l_{calc}^*	d_{calc}^{**}	hkl	l_{obs}	d_{obs}	l_{calc}^*	d_{calc}^{**}	hkl
5	9.31	4	9.27	110	5	2.007	3	2.007	732
		8	7.68	001	5	1.980	4	1.980	533
20	6.57	28	6.57	201	5	1.968	6	1.965	800
10	4.80	7	4.81	311	5	1.950	4	1.950	203
		3	4.77	310			2	1.937	730
10	4.64	8	4.64	220	5	1.931	3	1.933	152
30	4.33	41	4.32	221			2	1.927	352
5	4.22	8	4.21	401	5	1.908	2	1.907	551
		3	3.45	221	5	1.869	6	1.869	912
5	3.41	5	3.42	712			4	1.854	550
		3	3.40	421	5	1.852	5	1.850	243
		7	3.39	312	5	1.833	6	1.830	404
5	3.34	4	3.34	002			2	1.816	552
		3	3.34	311	10	1.762	11	1.762	043
5	3.28	2	3.28	511	5	1.745	4	1.744	913
		6	3.24	402	5	1.727	3	1.727	641
30	3.121	33	3.126	131	5	1.696	8	1.695	262
		34	3.101	331	10	1.674	10	1.674	004
100	3.077	100	3.086	222	10	1.643	13	1.644	804
5	3.034	12	3.033	510	5	1.638	7	1.634	333
20	2.913	25	2.915	401	5	1.623	13	1.621	840
20	2.871	23	2.870	040	5	1.614	7	1.613	243
		10	2.864	601	5	1.600	5	1.602	933
5	2.709	1	2.711	202			6	1.591	661
10	2.638	16	2.638	041	20	1.589	20	1.587	843
		8	2.615	132	5	1.565	1	1.565	734
10	2.604	12	2.599	421	10	1.544	10	1.543	444
10	2.563	20	2.563	621			1	1.491	172
10	2.452	21	2.451	222	5	1.489	2	1.488	372
		23	2.404	622	10	1.470	5	1.469	732
40	2.400	17	2.395	711			5	1.468	841
		9	2.398	241	5	1.458	2	1.456	10,4,1
5	2.366	4	2.372	441	5	1.447	3	1.445	443
		10	2.362	312	20	1.436	19	1.435	080
		1	2.233	003	5	1.422	5	1.420	11,3,1
5	2.235	4	2.230	223	5	1.410	2	1.410	625
5	2.205	2	2.204	710	5	1.394	3	1.394	623
10	2.179	15	2.179	042	5	1.364	4	1.362	771
		9	2.162	442	5	1.358	4	1.356	372
10	2.159	7	2.155	402	5	1.301	5	1.300	842
5	2.132	5	2.133	801	10	1.283	3	1.282	951
		6	2.114	151			4	1.281	12,4,2
		5	2.048	623	5	1.257	2	1.256	12,4,1
5	2.045	9	2.045	441	5	1.242	1	1.240	972
		4	2.042	332	5	1.222	1	1.224	135
10	2.026	5	2.027	641	5	1.202	4	1.201	12,4,4
5	2.021	1	2.019	713	5	1.195	5	1.193	626

* Calculated from crystal-structure refinement using SHELXTL XPOW (Sheldrick, 1990).

** Calculated from cell parameters refined from powder diffraction data: $a = 17.188(4)$, $b = 11.477(8)$, $c = 7.322(5)$ Å, $\beta = 113.83(4)^\circ$.

$R = 3.8\%$, with isotropic temperature factors. The final steps of the least squares refinement involved a conversion to anisotropic temperature factors and the location of the four H atoms that correspond to density maxima of approximately one electron on the difference Fourier map. The final residual indices were $R = 2.6\%$ and $R_w = 2.3\%$. Peak maxima and minima on the final difference map were less than one-half electron. Table 4 contains the final positional and thermal parameters. Selected interatomic distances and angles are given in Table 5. The observed and calculated structure factors (Table 6) have been deposited.¹

¹ A listing of the observed and calculated structure factors (Table 6) may be ordered as Document AM-92-512 from the Business Office, Mineralogical Society of America, 1130 Seventeenth Street NW, Suite 330, Washington, DC 20036, U.S.A. Please remit \$5.00 in advance for the microfiche.

The crystal structure of attakolite was also refined in the two possible noncentrosymmetric space groups $C2$ and Cm , but neither refinement indicated any significant improvement. Thus the discussion below is for the centrosymmetric structure only.

DESCRIPTION AND DISCUSSION OF THE STRUCTURE

For the refined attakolite structure, bond valence sums calculated using the parameters of Brown (1981) are [8] (Ca,Sr) 1.83 or [10] (Ca,Sr) 1.94, Mn 2.00, Al1 3.08, Al2 3.04, (Si,P) 4.31, P1 4.94, P2 5.05, O1 1.85, O2 1.83, O3 1.79, O4 1.96, O5 1.96, O6 2.02, O7 1.85, O8 2.01, O9 2.06, O11 1.13, O12 1.19, O13 1.23, and O14 1.50 vu. These bond valence sums indicate that the Ca site has tenfold coordination even though two of the bond lengths (3.249 Å) are quite long. They confirm Mn as divalent. P substitutes for Si, and with the atomic proportions of

TABLE 4. Positional and anisotropic thermal parameters ($\times 100, \text{\AA}^2$) for atakolite

Atom	x	y	z	U_{11}	U_{22}	U_{33}	U_{23}	U_{13}	U_{12}	U_{eq}
Ca	0	0.2592(1)	0	1.09(3)	1.46(3)	1.01(2)	0	0.63(2)	0	1.12(2)
Mn	0.2870(1)	0	0.0488(1)	0.54(2)	1.16(3)	1.25(93)	0	0.13(2)	0	1.06(2)
Al1	0.1329(1)	0.3670(1)	0.4964(1)	0.71(4)	0.58(4)	0.71(4)	0.06(3)	0.27(3)	-0.09(3)	0.61(2)
Al2	0.1190(1)	0.1292(1)	0.7685(1)	0.68(4)	0.60(4)	0.64(4)	0.00(3)	0.24(3)	-0.06(3)	0.61(2)
Si	0.0515(1)	0	0.3308(1)	0.62(4)	0.61(4)	0.57(4)	0	0.20(3)	0	0.62(3)
P1	0.4664(1)	0	0.2349(1)	0.61(4)	0.71(4)	0.70(4)	0	0.30(3)	0	0.66(3)
P2	0.2094(1)	0.2534(1)	0.1948(1)	0.56(2)	0.57(3)	0.60(2)	-0.03(2)	0.2512	-0.01(2)	0.57(2)
O1	0.4068(2)	0	0.3532(4)	0.8(1)	1.2(1)	1.1(1)	0	0.56(9)	0	1.00(8)
O2	0.4045(2)	0	0.0169(4)	1.0(1)	1.8(1)	0.8(1)	0	0.27(9)	0	1.23(8)
O3	-0.0057(1)	-0.1135(2)	0.2474(2)	0.81(7)	0.82(9)	0.91(8)	-0.03(6)	0.30(6)	-0.02(7)	0.86(6)
O4	0.2691(1)	0.1472(2)	0.2618(2)	0.70(7)	0.72(8)	0.73(7)	-0.05(6)	0.20(6)	0.13(6)	0.75(5)
O5	0.2621(1)	0.3610(2)	0.1893(2)	0.83(7)	0.76(8)	1.12(8)	0.09(7)	0.41(6)	-0.06(7)	0.90(6)
O6	0.1629(1)	0.2742(2)	0.3297(2)	1.18(8)	1.04(9)	1.19(8)	-0.16(7)	0.84(7)	-0.06(6)	1.02(6)
O7	0.0948(2)	0	-0.4268(4)	1.1(1)	0.7(1)	0.9(1)	0	0.4(1)	0	0.90(8)
O8	0.5228(1)	-0.1091(2)	0.2854(2)	0.79(8)	0.76(8)	1.13(8)	-0.01(7)	0.34(7)	0.10(6)	0.91(6)
O9	0.1395(1)	0.2315(2)	-0.0145(2)	0.78(7)	0.96(9)	0.74(7)	-0.12(7)	0.18(6)	0.06(6)	0.86(5)
O11	0.1258(2)	0	0.2566(4)	1.5(1)	2.0(1)	1.2(1)	0	0.9(1)	0	1.50(9)
O12	0.1770(2)	1/2	0.4372(4)	1.2(1)	0.9(1)	0.9(1)	0	0.7(1)	0	0.91(8)
O13	0.0884(1)	0.2440(2)	0.5809(2)	0.51(8)	1.09(8)	0.70(8)	0.15(7)	0.04(6)	-0.19(7)	0.83(6)
O14	0.1546(2)	0	-0.0609(4)	1.0(1)	0.7(1)	0.6(1)	0	0.4(1)	0.8(1)	0.75(8)
H11	0.339(3)	1/2	-0.321(8)	3.0						
H12	0.682(3)	0	0.357(7)	3.0						
H13	0.555(2)	-0.226(4)	0.510(5)	3.0						
H14	0.152(3)	0	0.021(8)	3.0						

Note: Temperature factors are of the form $\exp[-2\pi^2(U_{11}V_{11}h^2a^2 + U_{22}k^2b^2 + \dots + 2U_{12}hka^*b^*)]$. Estimated standard deviations are in parentheses.

the microprobe analysis of ($\text{Si}_{10.69}\text{P}_{0.31}$) the site valence of 4.31 vu is in good agreement with that calculated above. The O sites O11, O12, O13, and O14 give bond valence sums indicative of OH ions, and their respective H atoms

were located. It should be noted that the H-O bond distances listed in Table 5 range from 0.60 to 0.63 Å. These distances are considerably shorter than the distances of approximately 0.8 and 1.0 Å that are usually observed

TABLE 5. Selected interatomic distances (Å) and angles (°) for atakolite

Ca polyhedron				Mn polyhedron			
Ca-O3	2.497(2) × 2			Mn-O1	2.343(2)		
-O6	2.869(1) × 2			-O2	2.128(2)		
-O8	2.478(2) × 2			-O4	2.403(2) × 2		
-O9	2.466(2) × 2			O5	2.261(2) × 2		
-O2	3.249(2) × 2			-O14	2.087(3)		
Average ^(a) 2.712	^(b) 2.578			Average	2.269		
Al1 octahedron				Al2 octahedron			
Al1-O1	2.150(2)	O1-O4	86.1(1)	Al2-O3	1.915(2)	O3-O7	88.5(1)
-O4	1.893(1)	-O8	83.9(1)	-O5	1.945(2)	-O9	87.1(1)
-O6	1.844(2)	-O12	77.0(1)	-O7	1.985(1)	-O13	92.6(1)
-O8	1.918(2)	-O13	96.6(1)	-O9	1.891(2)	-O14	90.9(1)
-O12	1.836(2)	O4-O6	100.7(1)	-O13	1.822(2)	O5-O7	93.3(1)
-O13	1.831(2)	-O12	89.7(1)	-O14	1.877(2)	-O9	90.2(1)
Average	1.912	-O13	87.4(1)	Average	1.906	-O13	92.6(1)
		O6-O8	90.1(1)			-O14	84.3(1)
		-O12	94.2(1)			O7-O13	95.1(1)
		-O13	92.4(1)			-O14	78.6(1)
		O8-O12	93.4(1)			O7-O13	94.5(1)
		-O13	88.3(1)			-O14	92.0(1)
P1 tetrahedron				P2 tetrahedron			
P1-O1	1.586(3)	O1-O2	103.8(1)	P2-O4	1.543(2)	O4-O5	108.7(1)
-O2	1.517(2)	-O8	110.7(1) × 2	-O5	1.545(2)	-O6	112.1(1)
-O8	1.538(2) × 2	O2-O8	111.0(1) × 2	-O6	1.520(2)	-O9	109.8(1)
Average	1.545	O8-O8	109.4(1)	-O9	1.537(1)	O5-O6	111.1(1)
				Average	1.536	-O9	109.7(1)
						O6-O9	105.4(1)
Si tetrahedron				Bonds to H			
Si-O3	1.600(2) × 2	O3-O3'	109.4(1)	H11-O11	0.60(5)		
-O7	1.621(3)	-O7	110.9(1) × 2	H12-O12	0.63(6)		
-O11	1.579(4)	-O11	109.0(1) × 2	H13-O13	0.61(3)		
Average	1.600	O7-O11	107.3(1)	H14-O14	0.62(6)		
				H13...O3	2.25(4)		
				O13-O3	2.761(2)	O13-O3	143(5)
				H14...O11	1.95(6)		
				O11-O14	2.561(4)	O11-O14	170(6)

Note: Estimated standard deviations are in parentheses.

for structures determined with X-ray diffraction and neutron diffraction data, respectively, but such values are not unusual, owing to the high standard errors of H coordinates.

The attakolite structure consists of sheets of Al-octahedral chains cross linked by independent tetrahedra of Si and P (Fig. 1). The octahedral chains consist of edge-sharing dimers with apical connections at the tetrahedral links. Figure 1 shows how closely this planar feature of attakolite resembles that of carminite (Finney, 1963), which Moore and Araki (1975) point out is similar to palermoite. In attakolite, interstices in this layer are filled by Mn in sevenfold-coordinated polyhedral sites (capped octahedron) and by Ca in tenfold-coordinated polyhedral sites. In carminite, these two cation sites are both Pb in eightfold coordination, and in palermoite the interstices have either SrO_8 in a distorted cube or two tetrahedrally coordinated Li atoms.

In attakolite the chain is composed of $[\text{AlO}_4(\text{OH})_2]$ octahedra like that of palermoite, whereas in carminite the chain consists of $[\text{FeO}_4(\text{OH})_2]$ octahedra. In orthorhombic carminite there are two nonequivalent AsO_4 tetrahedra. Similarly there are two nonequivalent PO_4 tetrahedra in orthorhombic palermoite, but in attakolite the symmetry is reduced to monoclinic because of the presence of one $[\text{SiO}_3(\text{OH})]$ tetrahedron for every three PO_4 tetrahedra.

Tsumcorite, $\text{Pb}(\text{Zn},\text{Fe})_2(\text{AsO}_4)_2(\text{OH},\text{H}_2\text{O})_2$, is related to carminite, $\text{PbFe}_2^+(\text{AsO}_4)_2(\text{OH})_2$, both in chemical composition and in structure (Tillmanns and Gebert, 1973). In Figure 2 it can be seen that the octahedral chain is all edge sharing, in contrast to the alternating edge and apical sharing in the carminite octahedral chain (Fig. 1). This subtle but important shift is a direct result of the lowering of the cation valence in the octahedral site from essentially Fe^{3+} in carminite to Zn^{2+} in tsumcorite. The cross linking of the AsO_4 tetrahedra and Pb polyhedra is essentially the same in the two structures.

The octahedral chain and tetrahedral layer of tsumcorite are the same as those of the adelite and descloizite group minerals. Figure 2 shows the pyrobelonite structure (Donaldson and Barnes, 1955), a species of the descloizite group. The Pb atom that is in addition to that of tsumcorite is accommodated by a change in space group and an increase in cell volume. The descloizite group structure, space group $Pnma$, is essentially the same as that of the adelite group structure, space group $P2_12_12_1$, and it involves only a slight shift in atomic positions to reduce the symmetry to the noncentrosymmetric space group.

An interesting feature of the attakolite structure is the $[\text{HSiO}_4]$ anion, which is known to be an essential part of the pyroxenoid group structure, as well as other silicates, and has been described in the structures of the silicoarsenate, tiragalloite (Gramaccioli et al., 1979), and the silico-vanadate, medaite (Gramaccioli et al., 1981). In the crystal structures of tiragalloite, medaite, and attakolite the H atom bonds to the silicate anion rather than to the arsenate, vanadate, or phosphate anion, as predicted (Grice, 1991), because it is the stronger Lewis base. An

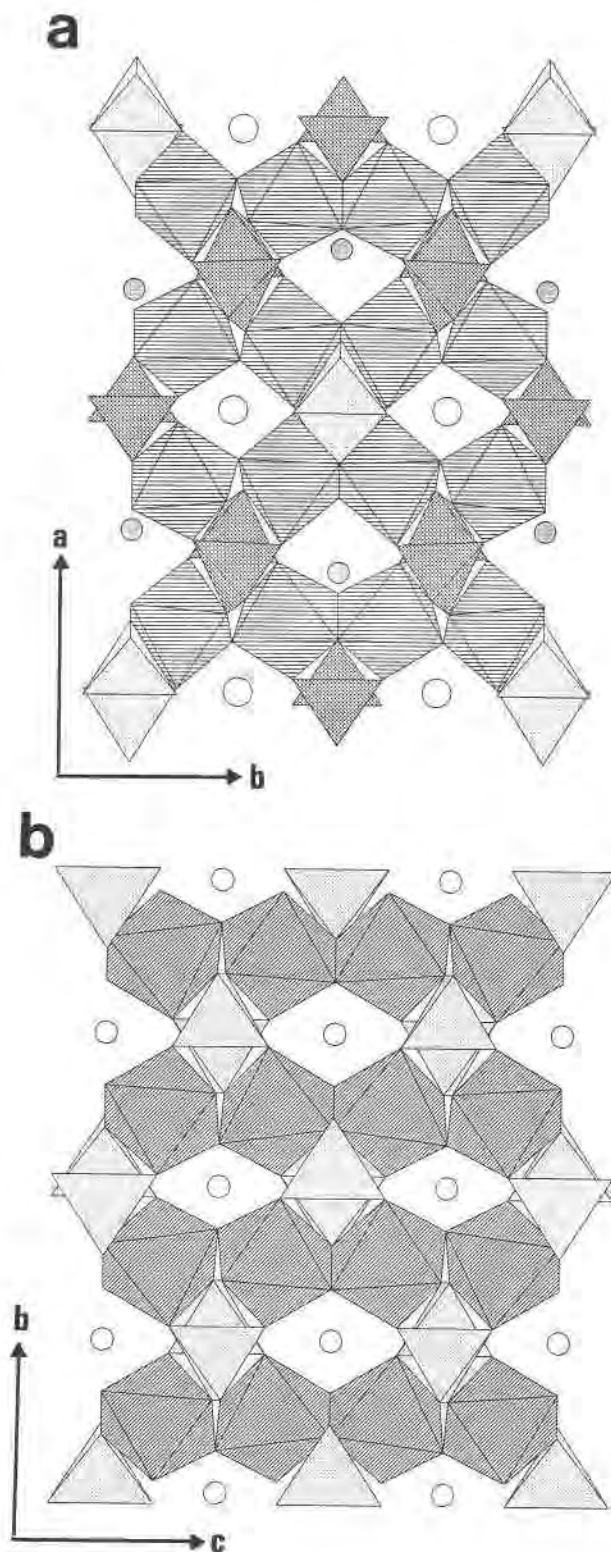


Fig. 1. (a) A [001] axis projection of the attakolite structure with Ca atoms as open circles, Mn atoms as shaded circles, apical and edge-sharing chains of Al octahedra, and tetrahedra of Si (light shading) and P (dark shading). (b) A b axis projection of the carminite structure with Pb atoms as open circles, attakolite-type chains of Fe octahedra and As tetrahedra.

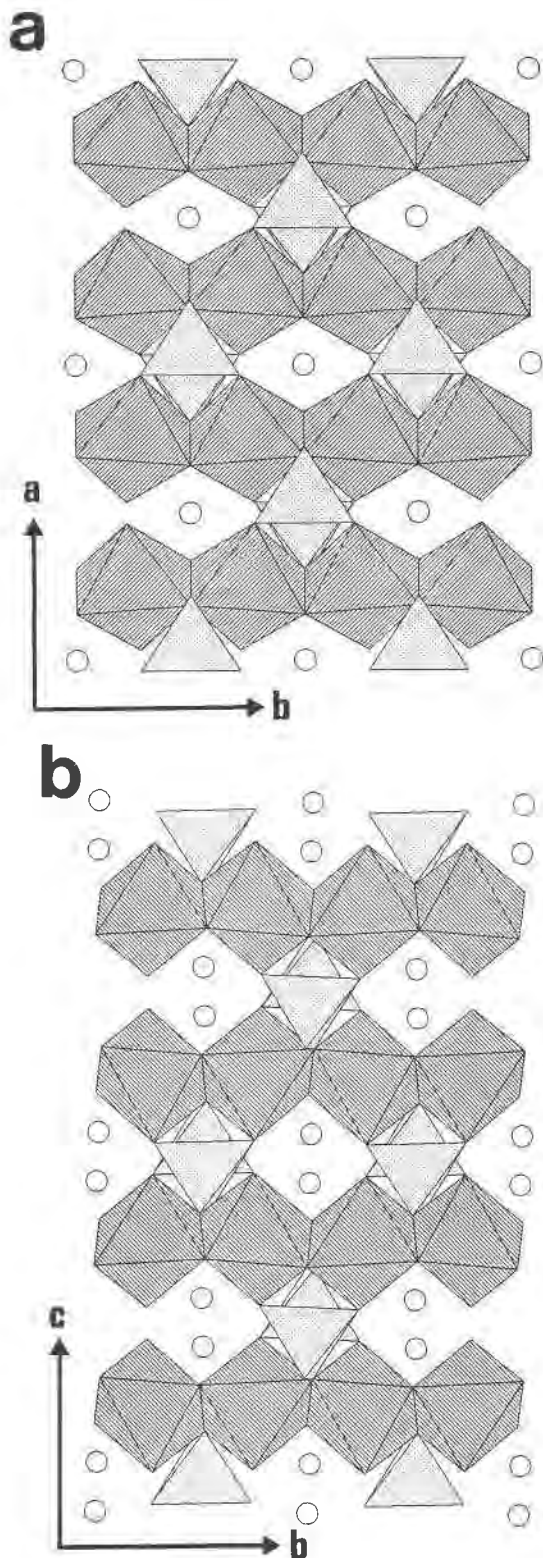


Fig. 2. (a) A [001] axis projection of the tsumcorite structure with Pb atoms as open circles, edge-sharing chains of Zn octahedra, and As tetrahedra. (b) An a axis projection of the pyrobelonite (descloizite group) structure with Pb atoms as open circles, edge-sharing chains of Mn octahedra and V tetrahedra.

interesting contradiction to this prediction is manifested in the crystal structure of ashburtonite (Grice et al., 1991), where the silicate anions polymerize into a tight four-membered ring in response to the highly electronegative Pb ion, leaving the carbonate group as the stronger Lewis base in the complex and thereby forming a bicarbonate ion.

Although very few silico-phosphate crystal structures have been determined, it appears that their structural topology resembles much more that of phosphates, arsenates, and vanadates than that of silicates; hence they would be more appropriately grouped in the former classification.

ACKNOWLEDGMENTS

The authors are grateful to the following for their continued cooperation and support: F.C. Hawthorne, University of Manitoba, for generously allowing the use of the single-crystal diffractometer, and Lisa Wong and Denise Groulx, Canadian Museum of Nature, for the typing of this manuscript. We would also like to thank the referees, C.M. Gramacciolo, T. Pilati, and E. Tillmanns and the Associate Editor T. Armbruster for their helpful suggestions and corrections, which greatly improved the manuscript.

REFERENCES CITED

- Blomstrand, C.W. (1868) Om Westanå mineralier. Öfversigt Akademien Förhandlingar, Kungliga Svenska Vetenskapsakademien, 25, 197
- Brown, I.D. (1981) The bond valence method: An empirical approach to chemical structure and bonding. In M. O'Keefe and A. Navrotsky, Eds., *Structure and bonding in crystals*, vol. II, p. 1-30. Academic Press, New York.
- Cromer, D.T., and Liberman, D. (1970) Relativistic calculation of anomalous scattering factors for X-rays. *Journal of Chemical Physics*, 53, 1891-1898
- Cromer, D.T., and Mann, J.B. (1968) X-ray scattering factors computed from numerical Hartree-Fock wave functions. *Acta Crystallographica*, A24, 321-324.
- Donaldson, D.M., and Barnes, W.H. (1955) The structures of the minerals of the descloizite and adelite groups: II—pyrobelonite. *American Mineralogist*, 40, 580-596.
- Finney, J.J. (1963) The crystal structure of carminite. *American Mineralogist*, 48, 1-13.
- Gabrielson, O., and Geijer, P. (1965) The mineral attackolite. *Arkiv för Mineralogi och Geologi*, 3, 537-543
- Gramaccioli, C.M., Pilati, T., and Liborio, G. (1979) The nature of a manganese (II) arsenatotrisilicate, $Mn_4[AsSi_3O_{12}(OH)]$: The presence of a new tetrapolyphosphate-like anion. *Acta Crystallographica*, B35, 2287-2291.
- Gramaccioli, C.M., Liborio, G., and Pilati, T. (1981) Structure of medaite, $Mn_4[VSi_3O_{12}(OH)]$: The presence of a new kind of heteropolysilicate anion. *Acta Crystallographica*, B37, 1972-1978.
- Grice, J.D. (1991) Bicarbonate minerals: Crystal chemistry and geological significance. *Geological Association of Canada Program and Abstracts*, 16, A47
- Grice, J.D., Nickel, E.H., and Gault, R.A. (1991) Ashburtonite, a new bicarbonate-silicate mineral from Ashburton Downs, Western Australia: Description and structure determination. *American Mineralogist*, 76, 1701-1707.
- Mead, C.W., and Mrose, M.E. (1968) Solving problems in phosphate mineralogy with the electron probe. *U.S. Geological Survey Professional Paper*, 600-D, D204-D206.
- Moore, P.B., and Araki, T. (1975) Palermoite, $SrLi_2[Al_2(OH)_2(PO_4)_2]$: Its atomic arrangement and relationship to carminite, $Pb_2[Fe_2(OH)_2(AsO_4)_2]$. *American Mineralogist*, 60, 460-465.
- North, A.C.T., Phillips, D.C., and Mathews, F.S. (1968) A semi-empirical method of absorption correction. *Acta Crystallographica*, A24, 351-359.

- Palache, C., Berman, H., and Frondel, C. (1951) The system of mineralogy, vol. 2 (7th edition), p. 845. Wiley, New York.
- Sheldrick, G.M. (1990) SHELXTL, a crystallographic computing package, revision 4.1. Siemens Analytical X-Ray Instruments, Inc., Madison, Wisconsin.
- Tillmanns, E., and Gebert, W. (1973) The crystal structure of tsumcorite, a new mineral from Tsumeb mine, S.W. Africa. *Acta Crystallographica*, B29, 2789–2794.

MANUSCRIPT RECEIVED SEPTEMBER 17, 1991

MANUSCRIPT ACCEPTED JULY 14, 1992